Lithos 204 (2014) 14–19

Contents lists available at ScienceDirect

Lithos

journal homepage: www.elsevier.com/locate/lithos

CA-TIMS zircon U–Pb dating of felsic ignimbrite from the Binchuan section: Implications for the termination age of Emeishan large igneous province

Yu-Ting Zhong [a,b], Bin He [a], Roland Mundil [c], Yi-Gang Xu [a,*]

[a] State Key Laboratory of Isotope Geochemistry, Guangzhou Institute of Geochemistry, Chinese Academy of Sciences, Guangzhou 510640, China
[b] Graduate University of Chinese Academy of Sciences, Beijing 100049, China
[c] Berkeley Geochronology Center, Berkeley, CA 94709, USA

ARTICLE INFO

Article history:
Received 17 October 2013
Accepted 3 March 2014
Available online 12 March 2014

Keywords:
Zircon U–Pb geochronology
CA-TIMS
Felsic ignimbrite
Emeishan large igneous province
Guadalupian–Lopingian boundary
SW China

ABSTRACT

The age of the Emeishan lavas in SW China remains poorly constrained because the extrusive rocks are (1) thermally overprinted and so represent an open system unsuitable for $^{40}Ar/^{39}Ar$ geochronology and (2) in most cases devoid of zircon so that it is impossible for the application of U–Pb geochronology. Existing radiometric age constraints of Emeishan large igneous province are mainly from the application of SIMS and LA-ICP-MS U–Pb techniques to zircons from mafic and felsic intrusions, which represent indirect constraints for the lavas. In an attempt to directly determine the age of the Emeishan lava succession, high-resolution chemical abrasion-thermal ionization mass spectrometry (CA-TIMS) zircon U–Pb techniques have been used on the felsic ignimbrite at the uppermost part of the Emeishan lava succession. These techniques have yielded a weighted mean $^{206}Pb/^{238}U$ age of 259.1 ± 0.5 Ma (n = 6; MSWD = 0.7). We interpret this age as the termination age of the Emeishan flood basalts. The age of the Guadalupian–Lopingian boundary is still unconstrained by high-resolution geochronology but is likely to be close to our new age for this felsic ignimbrite.

© 2014 Elsevier B.V. All rights reserved.

1. Introduction

Numerous studies suggest a causal link between large igneous provinces (LIPs) and mass extinctions and/or global environmental changes in the history of the Earth (e.g., Courtillot and Renne, 2003; Wignall, 2001). Evidence for a temporal link comes mainly from high-resolution geochronology from both LIP products and altered claystones within fossil-bearing strata that record extinctions. The most striking example is the temporal coincidence of the Siberian Traps and the Permian–Triassic mass extinction (Bowring et al., 1998; Mundil et al., 2004; Reichow et al., 2009; Renne et al., 1995; Shen et al., 2011). It is therefore evident that the accurate geochronology of LIPs is pivotal in understanding both their geodynamic context as well as potential causal links with biotic crises (Courtillot and Renne, 2003; Wignall, 2001).

Despite numerous geochemical, paleontological, paleomagnetic, geophysical, and geochronological research on the Emeishan LIP (e.g., Ali et al., 2004; Chung and Jahn, 1995; He et al., 2003, 2007; Xiao et al., 2004a; Xu et al., 2001, 2004, 2008, 2010; Zhou et al., 2002), the age of the lavas is still debated (Shellnutt, in press; Shellnutt et al., 2012). Although the Emeishan LIP has been dated by $^{40}Ar/^{39}Ar$ and U–Pb techniques, many of the $^{40}Ar/^{39}Ar$ dating results yield Mesozoic–Cenozoic ages (Ali et al., 2004; Lo et al., 2002), most likely as a result of open system behavior of the analyzed minerals and rocks due to Mesozoic and Cenozoic thermotectonic events in the western Yangtze Block. Consequently, the timing of the Emeishan LIP magmatism is mainly constrained by U–Pb zircon dates from mafic–ultramafic and felsic intrusions (e.g., Shellnutt et al., 2012; Xu et al., 2008; Zhong et al., 2007, 2009, 2011; Zhou et al., 2002). It is assumed that these intrusive bodies are genetically related to the Emeishan LIP, and the acquired U–Pb ages imply that the main phase of the Emeishan LIP took place at ~257–260 Ma (Shellnutt et al., 2012; Xu et al., 2008; Zhou et al., 2002). This age is broadly consistent with the stratigraphic constraints that place the Emeishan basalts between the Middle and the Late Permian, around the Guadalupian–Lopingian (G–L) boundary (259.8 ± 0.4 Ma; Henderson et al., 2012).

Constraints for both the age and, in particular, the duration of the Emeishan volcanism are therefore still scarce and controversial. This is further complicated by ambiguous structural relationships of intrusions and mafic sills and dykes with respect to the extrusive rocks. It is unclear that the Emeishan volcanic event represents a single event or multiple phases of magmatism. This problem was partly resolved by He et al. (2007) who dated detrital zircon crystals by Sensitive High Resolution Ion Microprobe (SHRIMP) U–Pb methods from the clastic rocks from the Xuanwei Formation. He et al. (2007) demonstrated that these zircons (dated at 257 to 263 Ma) are mostly from acidic extrusives, which are the latest magmatic phase of the Emeishan LIP and so provides constraints on the termination age of the Emeishan volcanism.

* Corresponding author.
E-mail address: yigangxu@gig.ac.cn (Y.-G. Xu).

http://dx.doi.org/10.1016/j.lithos.2014.03.005
0024-4937/© 2014 Elsevier B.V. All rights reserved.

However, the SHRIMP techniques generally yield percent level uncertainty on individual spots analyses and 1–2% uncertainty on pooled ages but can be prone to inaccuracy if poorly calibrated or inhomogeneous standard materials are used or the calibration is inconsistent.

The application of TIMS zircon U–Pb techniques to chemically abraded single zircon crystals (CA-TIMS; Mattinson, 2005; Mundil et al., 2004) yields radiometric ages with superior precision and accuracy compared to those based on micro-beam analyses, i.e., Secondary Ion Mass Spectrometry (SIMS including SHRIMP) and Laser Ablation-Inductively Coupled Plasma-Mass Spectrometer (LA-ICP-MS) (Mundil et al., 2004; Shellnutt et al., 2012). In this study therefore, we use CA-TIMS to date zircons from the felsic ignimbrite in the uppermost part of the lava succession in the central part of the Emeishan LIP. The results yield a termination age for the Emeishan flood basalts that is in good agreement with the recently refined dates using the same method for the alkaline granitic plutons from the Emeishan LIP (Shellnutt et al., 2012). Potential implications of this age with regard to the G–L boundary age are also briefly discussed.

2. Geological background

The Emeishan LIP in SW China (Fig. 1a), which consists of flood basalts and contemporaneous mafic–ultramafic intrusions and felsic plutons, covers an area of more than 2.5×10^5 km^2 with a total thickness ranging from several hundred meters at the margin up to 5 km in the central area (Xu et al., 2001). Relatively limited exposure is likely due to erosion along the Ailaoshan–Red River fault and the Longmenshan

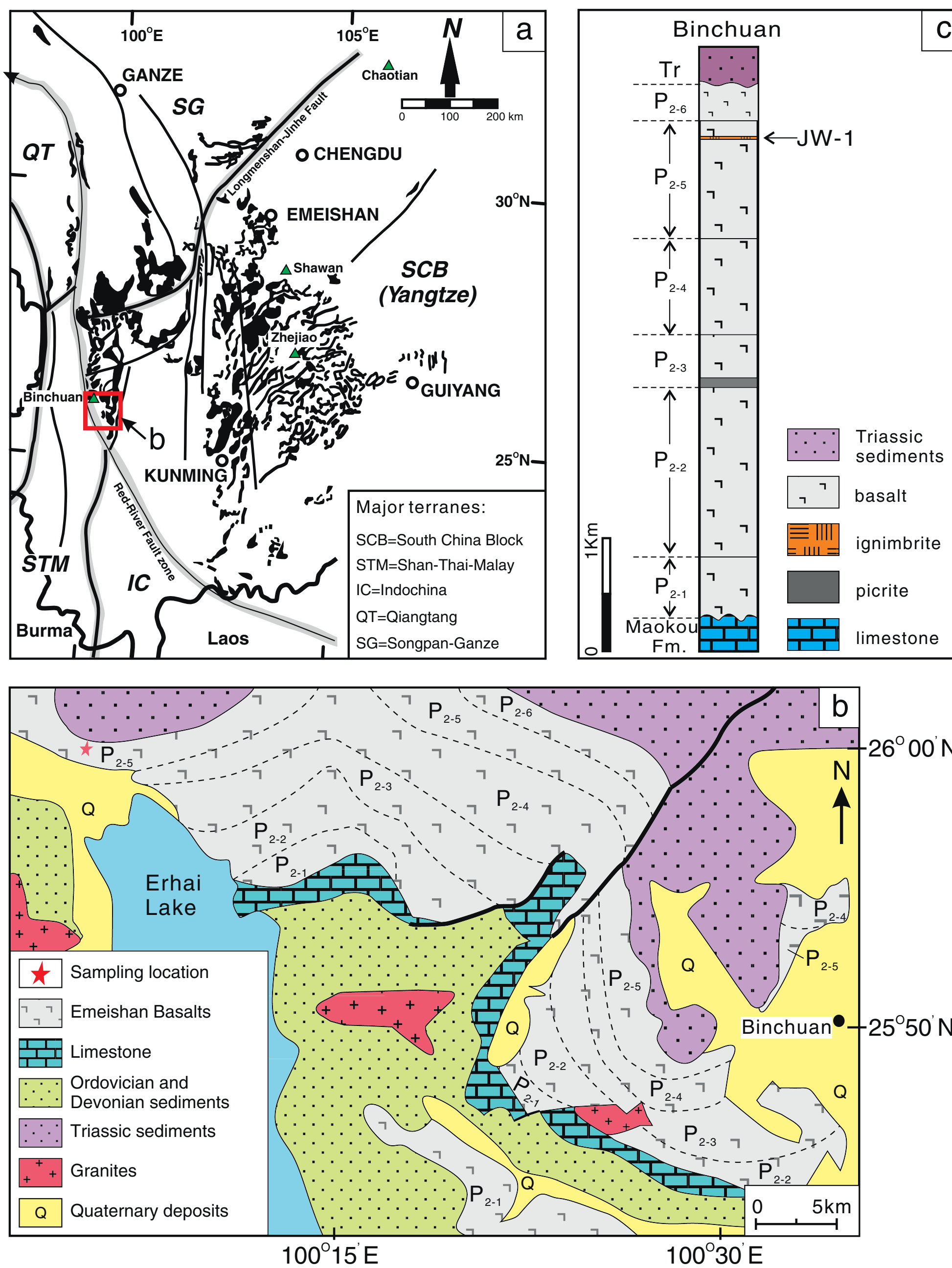

Fig. 1. (a) A schematic map showing the distribution of the Emeishan volcanic successions (after He et al., 2007). (b) A geological map showing the lava succession of the Emeishan LIP in the Binchuan area and sample locations. Note that $P_{2\text{-}1}$, $P_{2\text{-}2}$, $P_{2\text{-}3}$, $P_{2\text{-}4}$, $P_{2\text{-}5}$ and $P_{2\text{-}6}$ are sub-units of the Emeishan flood basalts. (c) A composite stratigraphic column showing the Emeishan lava succession in the Binchuan section and sample locations.

thrust belt (Xiao et al., 2004b) and subduction in the western Yangtze Block during the closure of the paleo-Tethys ocean (Liu et al., 2000).

The Emeishan lava succession comprises predominantly basaltic lavas and pyroclastic deposits, with minor amounts of picrite and basaltic andesite (Chung and Jahn, 1995; Song et al., 2001; Xu et al., 2001). In the eastern part of the Emeishan LIP, the succession clearly rests on the Middle Permian carbonates of the Maokou Formation and is directly overlain by the Upper Permian terrestrial clastic rocks of the Xuanwei Formation and the marine clastic rocks of the Longtan Formations (Jin and Shang, 2000). However, in most parts of the Emeishan LIP, the basalts are underlain by the Middle Permian Maokou Formation and are overlain by the Upper Triassic or Lower Triassic sedimentary rocks (Fig. 1b; He et al., 2007).

The Binchuan area was chosen for the current study because the Emeishan lava succession in this area appears to have a maximum thickness of about 5300 m (Xiao et al., 2004b), close to the central area. In addition, the absence of erosional soil beds in the thick Binchuan lava succession indicates a rapid eruption of the Emeishan volcanic rocks. The Binchuan composite section was divided into six sub-units (Fig. 1c, $P_{2\text{-}1}$ to $P_{2\text{-}6}$; Xiao et al., 2004a). The lower part of the lava succession (sub-units $P_{2\text{-}1}$ and $P_{2\text{-}2}$) consists mainly of aphyric and locally hyaloclastite lavas. The middle part (sub-units $P_{2\text{-}3}$ to $P_{2\text{-}4}$) includes more porphyritic basalts than the lower sub-units, whereas the upper basalts (sub-units $P_{2\text{-}5}$ and $P_{2\text{-}6}$) have higher phenocryst contents than those in the middle part. Several thin felsic volcanic rock layers are intercalated within the topmost part of sub-unit $P_{2\text{-}5}$ (Fig. 1c; He et al., 2007). These felsic volcanic rocks have not been documented in other parts of the LIP, probably due to extensive erosion in the central part of the Emeishan (He et al., 2003, 2007; Xu et al., 2004). The felsic volcanic layers in the uppermost part of the Binchuan section provide a rare, but excellent, opportunity to constrain the upper age of the Emeishan LIP.

3. Sampling and analytical methods

A felsic ignimbrite sample (JW-1) was taken from an interbedded felsic volcanic rock layer with a thickness of ~6.5 m within the uppermost unit of the Emeishan basalts in the Binchuan section which is located in the town of Jiangwei in the Yunnan Province (25°59′19.50″N, 100°7′21.78″E) (Fig. 1). Zircons separated from this sample have been previously dated by SHRIMP techniques to be 263 ± 4 Ma (He et al., 2007).

Sample preparation, chemical processing and CA-TIMS zircon U–Pb analyses were carried out at the Berkeley Geochronology Center. The sample was crushed and milled, and the powder was wet-sieved to remove the ultra-fine fraction. The nonmagnetic fraction of the resulting powder was separated by a Frantz Isodynamic Separator being put through a heavy liquid density separation. Zircons were microscopically inspected and euhedral crystals were selected for analyses. Zircon crystals were pretreated using the method of thermal annealing at 850 °C for 48 h, followed by chemical abrasion with conc. HF in pressurized dissolution capsules at 220 °C for 8 to 10 h to minimize the effects from Pb loss (Mattinson, 2005; Mundil et al., 2004). Crystals were selected based on clarity and apparent absence of inherited cores, and photomicrographs were taken to make estimates of grain weight and, ultimately, U and Th concentrations. Analytical procedures follow those described in Mundil et al. (2004). Comparison of the age results is facilitated by inter-laboratory cross calibration (Black et al., 2003, 2004) and analyses of reference materials (Mundil et al., 2004) as well as analyses of calibration solution distributed by the EARTHTIME initiative (preliminary BGC results are published in Irmis et al., 2011).

4. Results

Sample JW-1 is a fine-grained felsic ignimbrite and contains euhedral long prismatic zircons. Analyses of six individual zircons yield a coherent cluster with a weighted mean $^{206}Pb/^{238}U$ age of 259.1 ± 0.5 Ma (MSWD = 0.7) (Fig. 2). Th/U of the zircon crystals is within a narrow range of 0.55 to 0.65, indicating a uniform population (Table 1). The age is interpreted to represent the mean crystallization age of the magmatic zircon population and it is consistent with, but more precise than the age obtained from previous SHRIMP zircon U–Pb age (263 ± 4 Ma, MSWD = 7.5) reported by He et al. (2007).

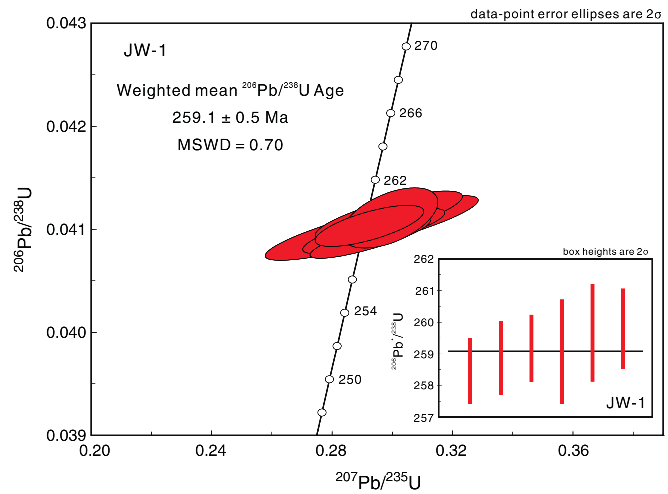

Fig. 2. Concordia plot for the felsic ignimbrite sample (JW-1) from the Binchuan section. Inset showing the $^{206}Pb/^{238}U$ ages of individual zircon crystals. Data were computed and plotted using the Isoplot 3.6 (Ludwig, 2008).

5. Discussion

5.1. Age of the Emeishan volcanism

In the past two decades numerous studies have sought to constrain the age and duration of the Emeishan LIP. Various dating techniques were used and have yielded more than 50 radiometric ages ranging from ~235 to ~271 Ma (summarized in Table 1 of Shellnutt, in press) (Fig. 3). A brief assessment of these published dates is given below:

Ages determined by micro-beam analytical techniques (i.e., SIMS and LA-ICP-MS) have constrained the intrusive magmatism of the Emeishan LIP as being similar to the Capitanian–Wuchiapingian boundary and the duration of the magmatism to be ~10 m.y. (Shellnutt et al., 2012). A coherent age of 259 ± 3 Ma has been obtained from SHRIMP zircon U–Pb dating for the Xinjie layered intrusion (Zhou et al., 2002). Assuming that the Xinjie intrusion represents a part of the feeder system of the Emeishan LIP, Zhou et al. (2002) suggested that the Emeishan LIP was emplaced at 259 ± 3 Ma. Guo et al. (2004) obtained a slightly older age of 262 ± 3 Ma for the zircons of mafic dykes that intruded Devonian strata in western Sichuan and they interpreted this age as the onset of the flood volcanism. Zhong and Zhu (2006) obtained a zircon U–Pb age of 259.3 ± 1.3 Ma for the Hongge intrusion, virtually identical within the error to that for the Panzhihua intrusion (Zhou et al., 2005). The Baimazhai intrusion in southern part of the Emeishan LIP has a SHRIMP zircon U–Pb age of 258.5 ± 3.6 Ma (Wang et al., 2006). Two ages of 260 ± 3 Ma and 258 ± 3 Ma have been obtained for the mafic–ultramafic intrusion in the Funing area (Zhou et al., 2006). Similar zircon U–Pb age (261 ± 4 Ma) was reported for the nepheline syenite in the Maomaogou area, the central Emeishan LIP (Luo et al., 2007). Recently, LA-ICP-MS zircon U–Pb analyses for the mafic–ultramafic intrusions and felsic plutons in the central part of the Emeishan LIP yielded ages ranging from 255.4 ± 3.1 Ma to 259.5 ± 2.7 Ma (Zhong et al., 2011). Although the obtained ages are overall consistent with each other, the age range permissible within their uncertainties is still ca. 10 m.y. (Fig. 3) if maximum error bounds are taken into consideration (Shellnutt et al., 2012). By contrast, the

Table 1
U–Pb isotopic data for the felsic ignimbrite sample (JW-1).

Sample	Cm. Pb (pg)	Th/U	$^{206}Pb/^{204}Pb$	$^{208}Pb/^{204}Pb$	$^{207}Pb/^{235}U$	2σ (%)	$^{206}Pb/^{238}U$	2σ (%)	ρ	$^{206}Pb^{*}/^{238}U$ (Ma)	2σ (abs.)	$^{207}Pb^{*}/^{235}U$ (Ma)	2σ (abs.)
01	0.9	0.58	294	88.6	0.2922	5.64	0.040908	0.4	0.83	258.46	1.02	260.3	14.68
02	1.1	0.55	188	67.5	0.2934	6.59	0.040974	0.44	0.81	258.87	1.14	261.2	17.2
03	1.2	0.59	234	77.9	0.2919	5.07	0.041023	0.4	0.71	259.17	1.04	260.1	13.18
04	1.2	0.57	131	58.4	0.2926	9.94	0.041005	0.63	0.86	259.06	1.63	260.6	25.92
05	1.1	0.65	298	94.8	0.2989	4.39	0.041102	0.58	0.52	259.66	1.52	265.5	11.66
06	1.2	0.64	179	70.2	0.2984	6.73	0.041123	0.48	0.78	259.79	1.25	265.2	17.84

Pb blank composition is $^{206}Pb/^{204}Pb = 18.55 \pm 0.63$, $^{207}Pb/^{204}Pb = 15.50 \pm 0.55$, $^{208}Pb/^{204}Pb = 38.07 \pm 1.56$, and a $^{206}Pb/^{204}Pb$–$^{207}Pb/^{204}Pb$ correlation of +0.9.
Present day Th/U ratio is calculated from radiogenic $^{208}Pb/^{206}Pb$ and age.
Isotopic ratios are corrected for tracer contribution and mass fractionation (0.15 ± 0.09%/amu).
Ratios of radiogenic Pb versus U are corrected for mass fractionation, tracer contribution and common Pb contribution.
ρ is correlation coefficient of radiogenic $^{207}Pb/^{235}U$ versus $^{206}Pb/^{238}U$.
Uncertainties of individual ratios and ages are given at the 2σ level and do not include decay constant errors.
Ratios involving ^{206}Pb are corrected for initial disequilibrium in $^{230}Th/^{238}U$ adopting Th/U = 6 for the crystallization environment, resulting in a correction of 80–90 ky.

magnetostratigraphic data and field observations indicate that the whole volcanic sequence formed within 1–2 m.y. (Ali et al., 2002; Zheng et al., 2010).

The ID-TIMS zircon U–Pb dating method benefits from superior precision although its spatial resolution is limited to entire crystals or fragments and thus it has limited applicability when complex zircon crystals comprising inherited cores are analyzed. On the other hand,

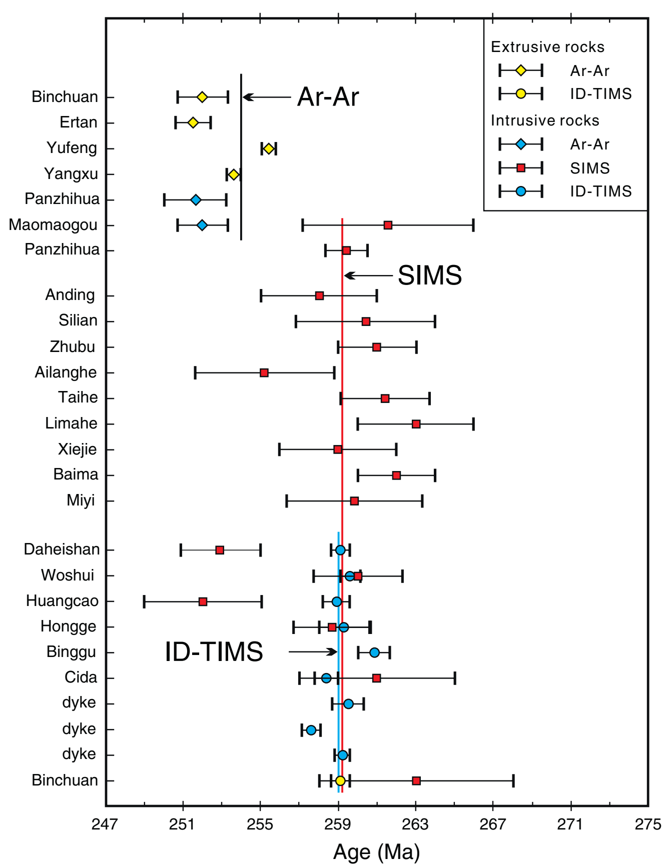

Fig. 3. A summary plot showing the representative published ages for the extrusive and intrusive rocks of Emeishan LIP using different techniques. Data compiled from Lo et al. (2002), Zhou et al. (2002, 2006, 2008), Fan et al. (2004), Zhong and Zhu (2006), He et al. (2007), Luo et al. (2007), Shellnutt and Zhou (2007), Zhong et al. (2007, 2011), Xu et al. (2008), Shellnutt et al. (2012) and this study. Vertical black, red and blue lines denote the weighted mean ages determined by Ar–Ar, SIMS and ID-TIMS, respectively. Note that SIMS and ID-TIMS methods yield essentially similar weighted mean ages with a superior analytical precision of the ID-TIMS method, whereas the $^{40}Ar/^{39}Ar$ ages underestimate the emplacement age of the igneous rocks in the Emeishan LIP.

the 'chemical abrasion' pretreatment method minimizes the effects of Pb loss, which usually lead to spuriously younger ages (Mattinson, 2005; Mundil et al., 2004). The pretreatment could remove the metamict portions within zircon crystals prior to analysis (Mattinson, 2005). Using CA-TIMS method, Shellnutt et al. (2012) obtained ages on several syenitic and granitic plutons and mafic dykes in the Panxi region, central part of the Emeishan LIP. Most of the results cluster at ~259 Ma with uncertainties of ±1 Ma (Fig. 3) and the magmatism in the Emeishan LIP was constrained to an interval from ~257 to ~260 Ma (Shellnutt et al., 2012). The limited duration of Emeishan magmatism is relatively short to the previous suggested ca. 10 m.y. (Xu et al., 2008; Zhong et al., 2011). Nevertheless, whether this age interval observed for the intrusive rocks is applicable to that for extrusive rocks remains unclear.

The duration of the Emeishan volcanism could be determined by directly dating the extrusive products throughout the basaltic piles. Unfortunately, the $^{40}Ar/^{39}Ar$ isotopic dating technique proved to be inapplicable for the Emeishan LIP due to the post-eruption alteration and thermotectonic resetting of the basalts (Ali et al., 2004; Lo et al., 2002). Basalts can alternatively be dated by zircon U–Pb methods but are very scarce because Zr is undersaturated in most basaltic magmas. No U-bearing minerals have been isolated from extrusive products of the Emeishan LIP. Zircon has only been found in thin interbedded felsic volcanic rock layers such as that analyzed in this study. Given the thin felsic volcanic rock layers in the Binchuan section are at the topmost of the sub-unit P_{2-5}, the 259.1 ± 0.5 Ma that is acquired in this study may be interpreted as the termination age of the Emeishan flood basalts. This age is consistent with those obtained for the intrusive rocks (Fig. 3), and is very close to the G–L boundary age (259.8 ± 0.4 Ma) recently suggested by Henderson et al. (2012). It has been suggested that the main phase of the Emeishan volcanism most likely occurred at the G–L boundary (He et al., 2007). The available data therefore collectively indicate that the Emeishan LIP was emplaced at ~259 Ma, probably over a very short interval less than 1 Ma.

5.2. Implications for the age of the Guadalupian–Lopingian boundary

The G–L boundary is defined by the chronomorphocline from *Clarkina postbitteri hongshuiensis* to *Clarkina postbitteri postbitteri* at the Penglaitan section in Laibin, Guangxi Province, South China (Jin et al., 2006). This boundary is associated with major regression, widespread volcanism and mass extinction (Hallam and Wignall, 1999; Isozaki, 2009; Ota and Isozaki, 2006; Zhang et al., 2013; Zhou et al., 2002). However, the temporal relationship between the Emeishan volcanism and the end-Guadalupian mass extinction is still unresolved. Constraining the age of this boundary is therefore important but the radiometric ages of claystones near the G–L boundary at GSSP (Global Boundary Stratotype Section and Point) in the Penglaitan section have shown that these deposits are redeposited clastic rocks rather than acidic tuffs or ashes, and are thus not suitable for the age determination of the G–L boundary (Zhong et al., 2013).

An age of 259.8 ± 0.4 Ma has recently been suggested for the G–L boundary in the Geologic Time Scale (GTS) 2012. This age is inferred from interpolation (Henderson et al., 2012) between the ages of 265.3 ± 0.2 Ma from the base of Capitanian stage (Bowring et al., 1998) and 257.3 ± 0.3 Ma from the Wuchiapingian stage (Mundil et al., 2004). However, it is somewhat uncertain because the bracketing ages are widely spaced in time and the former age possibly prone to inaccuracy due to Pb loss. Among the six analyzed zircon fractions from the ash exposed on Nipple Hill, Guadalupe Mountains National Park, Texas (Bowring et al., 1998), five of them yield a weighted mean $^{206}Pb/^{238}U$ age of 265.3 ± 0.2 Ma (MSWD = 0.50) (Bowring et al., 1998), whereas one yields an age of 263.6 Ma, which is obviously younger due to Pb loss, and therefore, was rejected. Mundil et al. (2004) reported ages of two ash beds (SH01 and SH03; 259.1 ± 1.0 Ma and 260.8 ± 0.8 Ma, respectively) close to the G–L boundary in the Shangsi section (northern Sichuan) that are close to 260 Ma. Based on mineralogy, geochemistry and zircon Hf–O isotopes of the clay layers (our unpublished data), the samples SH01 and SH03 are not volcanic ashes, instead they are clastic rocks resulting from the erosion of the Emeishan LIP (He et al., 2007). Therefore, the age of SH03 from the Shangsi section (260.8 ± 0.8 Ma) may be a maximum age of the Emeishan volcanism rather than a depositional age. In summary, the age for the G–L boundary suggested by GTS2012 (Henderson et al., 2012) needs further constraints.

Previous studies by He et al. (2007, 2010) have shown that the G–L boundary claystones in SW China were mainly derived from the uppermost part of the lava succession in the central part of the Emeishan LIP. Specifically, the lowermost part of G–L boundary claystone bed, which is called as the Wangpo Bed in Chinese literature (Lu, 1956), may represent eroded materials of felsic extrusives in the uppermost part of the Emeishan LIP. Given the fact that the G–L boundary claystones are genetically related to the Emeishan felsic volcanism, it is reasonable to infer that the felsic member in the uppermost part of the Emeishan basalts (Xu et al., 2001), and the G–L boundary claystones at the base of the Wuchiapingian all lie on an isochron horizon (Fig. 4). If this hypothesis is correct and the erosion occurred shortly after the deposition, our new CA-TIMS age (259.1 ± 0.5 Ma) for the felsic ignimbrite sample in the Binchuan section may provide an indirect constraint on the age of the G–L boundary. It is also worth emphasizing that our new date is in good agreement with the age of the G–L boundary suggested by Shen et al. (2010).

6. Conclusions

The new, precise CA-TIMS zircon U–Pb age of the felsic ignimbrite at the top of the lava succession of the Emeishan LIP indicates that the termination age of the Emeishan flood basalts is 259.1 ± 0.5 Ma. The age is likely to be close to the age of the G–L boundary if the claystones near the G–L boundary have been eroded shortly after the emplacement of the Emeishan volcanism. However, the precise age of the G–L boundary and the duration of Emeishan flood basalts need further constraints.

Acknowledgments

We are grateful to J. Gregory Shellnutt and Kwan-Nang Pang for their constructive reviews and Christina Yan Wang for editorial handling, which substantially improved the paper. This research was supported by a National Basic Research Program of China (973 Program No. 2011CB808906 and 2011CB808905) and National Natural Science Foundation of China grant nos. 41273011 and 41173037, as well as National Science Foundation award 0923669 to RM. This is contribution no. IS-1843 from GIGCAS.

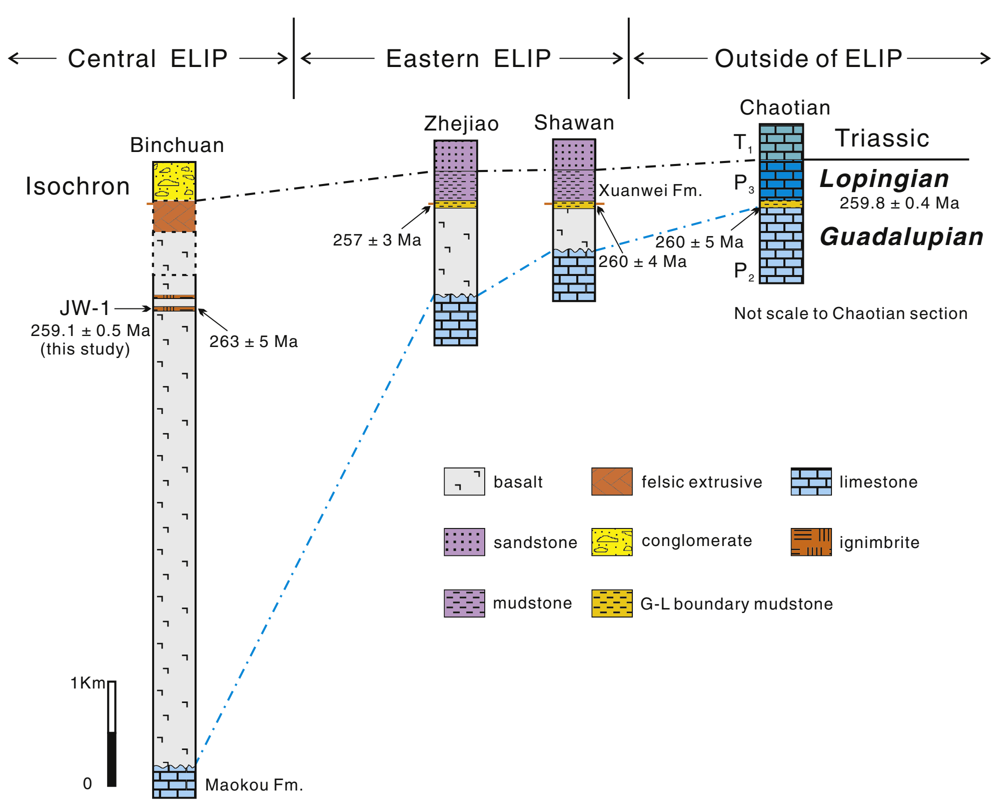

Fig. 4. Stratigraphic correlation among the sections in the central and eastern part of the Emeishan LIP and out with the LIP (modified after He et al., 2007). The red dash line marks the termination of the Emeishan flood basalts. The blue dashed and dot line indicates the onset of Emeishan flood magmatism.
Data sources: Guadalupian–Lopingian boundary age from Henderson et al. (2012), other ages from He et al. (2007).

References

Ali, J.R., Thompson, G.M., Song, X.Y., Wang, Y.L., 2002. Emeishan Basalts (SW China) and the 'end-Guadalupian' crisis: magnetobiostratigraphic constraints. Journal of the Geological Society 159, 21–29.

Ali, J.R., Lo, C.H., Thompson, G.M., Song, X.Y., 2004. Emeishan Basalts Ar–Ar overprint ages define several tectonic events that affected the western Yangtze platform in the Mesozoic and Cenozoic. Journal of Asian Earth Sciences 23, 163–178.

Black, L.P., Kamo, S.L., Williams, I.S., Mundil, R., Davis, D.W., Korsch, R.J., Foudoulis, C., 2003. The application of SHRIMP to Phanerozoic geochronology: a critical appraisal of four zircon standards. Chemical Geology 200, 171–188.

Black, L.P., Kamo, S.L., Allen, C.M., Davis, D.W., Aleinikoff, J.N., Valley, J.W., Mundil, R., Campbell, I.H., Korsch, R.J., Williams, I.S., Foudoulis, C., 2004. Improved $^{206}Pb/^{238}U$ microprobe geochronology by the monitoring of a trace-element-related matrix effect; SHRIMP, ID-TIMS, ELA-ICP-MS and oxygen isotope documentation for a series of zircon standards. Chemical Geology 205, 115–140.

Bowring, S.A., Erwin, D.H., Jin, Y.G., Martin, M.W., Davidek, E., Wang, W., 1998. U/Pb zircon geochronology and tempo of the end-Permian mass extinction. Science 280, 1039–1045.

Chung, S.L., Jahn, B.M., 1995. Plume–lithosphere interaction in generation of the EFB at the Permian–Triassic boundary. Geology 23, 889–892.

Courtillot, V.E., Renne, P.R., 2003. On the age of flood basalt events. Geoscience 335, 113–140.

Fan, W.M., Wang, Y.J., Peng, T.P., Miao, L.C., Guo, F., 2004. Ar–Ar and U–Pb chronology of Late Paleozoic basalts in western Guangxi and its constraints on the eruption age of the Emeishan basalt magmatism. Chinese Science Bulletin 49, 2318–2327.

Guo, F., Fan, W.M., Wang, Y.J., Li, C.W., 2004. When did the Emeishan plume activity start? Geochronological evidence from ultramafic–mafic dikes in Southwestern China. International Geologic Review 46, 226–234.

Hallam, A., Wignall, P.B., 1999. Mass extinctions and sea-level changes. Earth Science Reviews 48, 217–250.

He, B., Xu, Y.G., Chung, S.L., Xiao, L., Wang, Y.M., 2003. Sedimentary evidence for a rapid, kilometer scale crustal doming prior to the eruption of the EFB. Earth and Planetary Science Letters 213, 391–405.

He, B., Xu, Y.G., Huang, X.L., Luo, Z.Y., Shi, Y.R., Yang, Q.J., Yu, S.Y., 2007. Age and duration of the Emeishan flood volcanism, SW China: Geochemistry and SHRIMP zircon U–Pb dating of silicic ignimbrites, post-volcanic Xuanwei Formation and clay tuff at the Chaotian section. Earth and Planetary Science Letters 255, 306–323.

He, B., Xu, Y.G., Zhong, Y.T., Guan, J.P., 2010. The Guadalupian–Lopingian boundary mudstones at Chaotian (SW China) are clastic rocks rather than acidic tuffs: implication for a temporal coincidence between the end-Guadalupian mass extinction and the Emeishan volcanism. Lithos 119, 10–19.

Henderson, C.M., Davydiv, V.I., Wardlaw, B.R., 2012. The Permian period. In: Gradstein, F. M., Ogg, J.G., Schmitz, M.D., Ogg, G.M. (Eds.), The Geological Timescale 2012, vol. 2. Elsevier Press, Amsterdam, pp. 653–680.

Irmis, R.B., Mundil, R., Martz, J.W., Parker, W.G., 2011. High-resolution U–Pb ages from the upper Triassic Chinle formation (New Mexico, USA) support a diachronous rise of dinosaurs. Earth and Planetary Science Letters 309, 258–267.

Isozaki, Y., 2009. Illawarra reversal: the fingerprint of a superplume that triggered Pangean breakup and the end-Guadalupian (Permian) mass extinction. Gondwana Research 15, 421–432.

Jin, Y.G., Shang, Q.H., 2000. The Permian of China and its interregional correlation. In: Yin, H.F., Dickins, J.M., Shi, G.R., Tong, J. (Eds.), Permian–Triassic Evolution of Tethys and Western Circum-Pacific. Developments in Palaeontology and Stratigraphy, vol. 18. Elsevier Press, Amsterdam, pp. 71–98.

Jin, Y.G., Shen, S.Z., Henderson, C.M., Wang, X.D., Wang, W., Wang, Y., Cao, C.Q., Shang, Q. H., 2006. The Global Stratotype Section and Point (GSSP) for the boundary between the Capitanian and Wuchiapingian stage (Permian). Episodes 29, 253–262.

Liu, F.T., Liu, J.H., He, J.K., You, Q.Y., 2000. The subducted slab of the Yangtze continental block beneath the Tethyan orogen in the western Yunnan. Chinese Science Bulletin 45, 466–472.

Lo, C.H., Chung, S.L., Lee, T.Y., Wu, G.Y., 2002. Age of the Emeishan flood magmatism and relations to Permian–Triassic boundary events. Earth and Planetary Science Letters 198, 449–458.

Lu, Y.H., 1956. The Permian of Liangshan and its bearing on the classification and correlation of the Permian rocks of South China. Scientia Sinica 5, 733–761.

Ludwig, K.R., 2008. User's Manual for Isoplot 3.6. Berkeley Geochronology Center 1–77.

Luo, Z.Y., Xu, Y.G., He, B., Shi, Y.R., Huang, X.L., 2007. Geochronologic and petrochemical evidence for the genetic link between the Maomaogou nepheline syenites and the Emeishan large igneous province. Chinese Science Bulletin 52, 949–958.

Mattinson, J.M., 2005. Zircon U–Pb chemical abrasion ("CA-TIMS") method: combined annealing and multi-step partial dissolution analysis for improved precision and accuracy of zircon ages. Chemical Geology 220, 47–66.

Mundil, R., Ludwig, K.R., Metcalfe, I., Renne, P.R., 2004. Age and timing of the Permian mass extinctions: U/Pb dating of closed-system zircons. Science 305, 1760–1763.

Ota, A., Isozaki, Y., 2006. Fusiline biotic turnover across the Guadalupian-Lopingian (middle–upper Permian) boundary in mid-oceanic carbonate build-ups: biostratigraphy of accreted limestone in Japan. Journal of Asian Earth Sciences 26, 353–368.

Reichow, M.K., Pringle, M.S., Al'Mukhamedov, A.I., Allen, M.B., Andreichev, V.L., Buslov, M. M., Davies, C.E., Fedoseev, G.S., Fitton, J.G., Inger, S., Medvedev, A.Y., Mitchell, C., Puchkov, V.N., 2009. The timing and extent of the eruption of the Siberian Traps large igneous province: implications for the end-Permian environmental crisis. Earth and Planetary Science Letters 277, 9–20.

Renne, P.R., Zhang, Z.C., Richards, M.A., Black, M.T., Basu, A.R., 1995. Synchrony and causal relations between Permian–Triassic boundary crises and the Siberian flood volcanism. Science 269, 1413–1416.

Shellnutt, J.G., 2014. The Emeishan large igneous province: a synthesis. Geoscience Frontiers (in press).

Shellnutt, J.G., Zhou, M.F., 2007. Permian peralkaline, peraluminous and metaluminous A-type granites in the Panxi district, SW China: their relationship to the Emeishan mantle plume. Chemical Geology 243, 286–316.

Shellnutt, J.G., Denyszyn, S.W., Mundil, R., 2012. Precise age determination of mafic and felsic intrusive rocks from the Permian Emeishan large igneous province (SW China). Gondwana Research 22, 118–126.

Shen, S.Z., Henderson, C.M., Bowring, S.A., Cao, C.Q., Wang, Y., Wang, W., Zhang, H., Zhang, Y.C., Mu, L., 2010. High-resolution Lopingian (Late Permian) timescale of South China. Geological Journal 45, 122–134.

Shen, S.Z., Crowley, J.L., Wang, Y., Bowring, S.A., Erwin, D.H., Sadler, P.M., Cao, C.Q., Rothman, D.H., Henderson, C.M., Ramezani, J., Zhang, H., Shen, Y.A., Wang, X.D., Wang, W., Mu, L., Li, W.Z., Tang, Y.G., Liu, X.L., Liu, L.J., Zeng, Y., Jiang, Y.F., Jin, Y.G., 2011. Calibrating the end-Permian mass extinction. Science 334, 1367–1372.

Song, X.Y., Zhou, M.F., Hou, Z.Q., Cao, Z.M., Wang, Y., Li, Y., 2001. Geochemical constraints on the mantle source of the upper Permian Emeishan continental flood basalts, southwestern China. International Geology Review 43, 213–225.

Wang, C.Y., Zhou, M.F., Keays, R.R., 2006. Geochemical constraints on the origin of the Permian Baimazhai mafic–ultramafic intrusion, SW China. Contributions to Mineralogy and Petrology 152, 309–321.

Wignall, P.B., 2001. Large igneous provinces and mass extinctions. Earth Science Reviews 53, 1–33.

Xiao, L., Xu, Y.G., Mei, H.J., Zheng, Y.F., He, B., Pirajno, F., 2004a. Distinct mantle sources of low-Ti and high-Ti basalts from the western Emeishan large igneous province, SW China: implications for plume–lithosphere interaction. Earth and Planetary Science Letters 228, 525–546.

Xiao, L., Xu, Y.G., Xu, J.F., He, B., Franco, P., 2004b. Chemostratigraphy of flood basalts in the Garze–Litang region and Zongza block: implications for western extension of the Emeishan large igneous province, SW China. Acta Geologica Sinica 78, 61–67 (English Edition).

Xu, Y.G., Chung, S.L., Jahn, B.M., Wu, G.Y., 2001. Petrologic and geochemical constraints on the petrogenesis of Permian–Triassic EFB in southwestern China. Lithos 58, 145–168.

Xu, Y.G., He, B., Chung, S.L., Menzies, M.A., Frey, F.A., 2004. The geologic, geochemical and geophysical consequences of plume involvement in the Emeishan flood basalt province. Geology 30, 917–920.

Xu, Y.G., Luo, Z.Y., Huang, X.L., He, B., Xiao, L., Xie, L.W., Shi, Y.R., 2008. Zircon U–Pb and Hf isotope constraints on crustal melting associated with the Emeishan mantle plume. Geochimica et Cosmochimica Acta 72, 3084–3104.

Xu, Y.G., Chung, S.L., Shao, H., He, B., 2010. Silicic magmas from the Emeishan large igneous province, Southwest China: Petrogenesis and their link with the end-Guadalupian biological crisis. Lithos 119, 47–60.

Zhang, Y., Ren, Z.Y., Xu, Y.G., 2013. Sulfur in olivine-hosted melt inclusions from the Emeishan picrites: implications for S degassing and its impact on environment. Journal of Geophysical Research: Solid Earth 118, 4063–4070.

Zheng, L.D., Yang, Z.Y., Tong, Y.B., Yuan, W., 2010. Magnetostratigraphic constraints on two-stage eruptions of the Emeishan continental flood basalts. Geochemistry, Geophysics, Geosystems 11, Q12014.

Zhong, H., Zhu, W.G., 2006. Geochronology of layered mafic intrusions from the Pan-Xi area in the Emeishan large igneous province, SW China. Mineralium Deposita 41, 599–606.

Zhong, H., Zhu, W.G., Chu, Z.Y., He, D.F., Song, X.Y., 2007. SHRIMP U–Pb zircon geochronology, geochemistry, and Nd–Sr isotopic study of contrasting granites in the Emeishan large igneous province, SW China. Chemical Geology 236, 112–133.

Zhong, H., Zhu, W.G., Hu, R.Z., Xie, L.W., He, D.F., Liu, F., Chu, Z.Y., 2009. Zircon U–Pb age and Sr–Nd–Hf isotope geochemistry of the Panzhihua A-type syenitic intrusion in the Emeishan large igneous province, southwest China and implications for growth of juvenile crust. Lithos 110, 109–128.

Zhong, H., Campbell, I.H., Zhu, W.G., Allen, C.M., Hu, R.Z., Xie, L.W., He, D.F., 2011. Timing and source constraints on the relationship between mafic and felsic intrusions in the Emeishan large igneous province. Geochimica et Cosmochimica Acta 75, 1374–1395.

Zhong, Y.T., He, B., Xu, Y.G., 2013. Mineralogy and geochemistry of claystones from the Guadalupian-Lopingian boundary at Penglaitan, South China: insights into the pre-Lopingian geological events. Journal of Asian Earth Sciences 62, 438–462.

Zhou, M.F., Malpas, J., Song, X.Y., Robinson, P.T., Sun, M., Kennedy, A.K., Lesher, C.M., Keays, R.R., 2002. A temporal link between the Emeishan large igneous province (SW China) and the end-Guadalupian mass extinction. Earth and Planetary Science Letters 196, 113–122.

Zhou, M.F., Robinson, P.T., Lesher, C.M., Keays, R.R., Zhang, C.J., Malpas, J., 2005. Geochemistry, petrogenesis and metallogenesis of the Panzhihua gabbroic layered intrusion and associated Fe–Ti–V oxide deposits, Sichuan Province, SW China. Journal of Petrology 46, 2253–2280.

Zhou, M.F., Zhao, J.H., Qi, L., Su, W.C., Hu, R.Z., 2006. Zircon U–Pb geochronology and elemental and Sr–Nd isotope geochemistry of Permian mafic rocks in the Funing area, SW China. Contributions to Mineralogy and Petrology 151, 1–19.

Zhou, M.F., Arndt, N.T., Malpas, J., Wang, C.Y., Kennedy, A.K., 2008. Two magma series and associated ore deposit types in the Permian Emeishan large igneous province, SW China. Lithos 103, 352–368.